

Laboratory frame analysis of $e^+e^- \rightarrow \mu^+\mu^-$ scattering in the Noncommutative Standard Model

Prasanta Kumar Das^{1,*} and Abhishodh Prakash^{2,†}

¹*Birla Institute of Technology and Science-Pilani,*

K. K. Birla Goa campus, NH-17B, Zuarinagar, Goa-403726, India

²*Department of Physics and Astronomy,*

Stony Brook University, Stony Brook, New York 11790, USA

(Dated: December 3, 2024)

Abstract

We study the muon pair production $e^+e^- \rightarrow \mu^+\mu^-$ in the noncommutative extension of the standard model using the Seiberg-Witten maps of this to the second order of the noncommutative parameter $\Theta_{\mu\nu}$. Using $\mathcal{O}(\Theta^2)$ Feynman rules, we find the $\mathcal{O}(\Theta^4)$ cross section (with all other lower order contributions simply cancelled) for the pair production. The momentum dependent $\mathcal{O}(\Theta^2)$ NC interaction significantly modifies the cross section and angular distributions which are different from the standard model. We include the effects of earth's rotation in our analysis and plot several time-averaged and time dependent observables. In particular, the time-averaged azimuthal distribution of the cross section shows significant departure from the standard model distribution. We found strong dependence of the total cross section(time- averaged) on the orientation of the noncommutative electric vector ($\vec{\Theta}_E$). The periodic nature of the cross-section(un-averaged) with time over a complete day seems to be startling and can be thoroughly probed at the upcoming Linear Collider(LC).

*Author(corresponding) : pdas@bits-goa.ac.in

†Abhishodh.Prakash@stonybrook.edu

I. INTRODUCTION

Recently the TeV scale gravity scenario has drawn a lot of attention among the high energy physics community. In some brane-world models [1] where this TeV scale gravity is realized, one can principally expect to see some stringy effects in the upcoming TeV colliders and in addition the signature of space-time noncommutativity. Interests in the noncommutative(NC) field theory arose from the pioneering work by Snyder [2] and has been revived recently due to developments connected to string theories in which the noncommutativity of space-time is an important characteristic of D-brane dynamics at the low energy limit[3–5]. Although Douglas *et al.*[4] in their pioneering work have shown that the noncommutative field theory is a well-defined quantum field theory, the question that remains is whether the string theory prediction and the noncommutative effect can be seen at the energy scale attainable in present or near future experiments instead of the 4-*d* Planck scale M_{pl} . A notable work by Witten *et al.*[6] suggests that one can see some stringy effects by lowering the threshold value of commutativity to TeV, a scale which is not so far from present or future collider scale.

What is space-time noncommutativity? It means space and time no longer commute with each other. Now writing the space-time coordinates as operators we find

$$[\hat{X}_\mu, \hat{X}_\nu] = i\Theta_{\mu\nu} \quad (1)$$

where the matrix $\Theta_{\mu\nu}$ is real and antisymmetric. The NC parameter $\Theta_{\mu\nu}$ has dimension of area and reflects the extent to which the space-time coordinates are noncommutative i.e. fuzzy. Furthermore, introducing a NC scale Λ , we rewrite Eq. 1 as

$$[\hat{X}_\mu, \hat{X}_\nu] = \frac{i}{\Lambda^2} c_{\mu\nu} \quad (2)$$

where $\Theta_{\mu\nu}(= c_{\mu\nu}/\Lambda)$ and $c_{\mu\nu}$ has the same properties as $\Theta_{\mu\nu}$. To study an ordinary field theory in such a noncommutative fuzzy space, one replaces all ordinary products among the field variables with Moyal-Weyl(MW) [7] \star products defined by

$$(f \star g)(x) = \exp\left(\frac{1}{2}\Theta_{\mu\nu}\partial_{x^\mu}\partial_{y^\nu}\right) f(x)g(y)|_{y=x}. \quad (3)$$

Using this we find the noncommutative quantum electrodynamics(NCQED) Lagrangian as

$$\mathcal{L} = \frac{1}{2}i(\bar{\psi} \star \gamma^\mu D_\mu \psi - (D_\mu \bar{\psi}) \star \gamma^\mu \psi) - m\bar{\psi} \star \psi - \frac{1}{4}F_{\mu\nu} \star F^{\mu\nu}, \quad (4)$$

which are invariant under the following transformations

$$\psi(x, \Theta) \rightarrow \psi'(x, \Theta) = U \star \psi(x, \Theta), \quad (5)$$

$$A_\mu(x, \Theta) \rightarrow A'_\mu(x, \Theta) = U \star A_\mu(x, \Theta) \star U^{-1} + \frac{i}{e} U \star \partial_\mu U^{-1}, \quad (6)$$

where $U = (e^{i\Lambda})_\star$. In the NCQED Lagrangian [Eq.4] $D_\mu \psi = \partial_\mu \psi - ie A_\mu \star \psi$, $(D_\mu \bar{\psi}) = \partial_\mu \bar{\psi} + ie \bar{\psi} \star A_\mu$, and $F_{\mu\nu} = \partial_\mu A_\nu - \partial_\nu A_\mu - ie(A_\mu \star A_\nu - A_\nu \star A_\mu)$.

The alternative is the Seiberg-Witten(SW)[3–5, 8] approach in which both the gauge parameter Λ and the gauge field A^μ is expanded as

$$\Lambda_\alpha(x, \Theta) = \alpha(x) + \Theta^{\mu\nu} \Lambda_{\mu\nu}^{(1)}(x; \alpha) + \Theta^{\mu\nu} \Theta^{\eta\sigma} \Lambda_{\mu\nu\eta\sigma}^{(2)}(x; \alpha) + \dots \quad (7)$$

$$A_\rho(x, \Theta) = A_\rho(x) + \Theta^{\mu\nu} A_{\mu\nu\rho}^{(1)}(x) + \Theta^{\mu\nu} \Theta^{\eta\sigma} A_{\mu\nu\eta\sigma\rho}^{(2)}(x) + \dots \quad (8)$$

and when the field theory is expanded in terms of this power series Eq. (7) one ends up with an infinite tower of higher dimensional operators which renders the theory nonrenormalizable. However, the advantage is that this construction can be applied to any gauge theory with arbitrary matter representation. In the WM approach the group closure property is only found to hold for the $U(N)$ gauge theories and the matter content is found to be in the (anti)-fundamental and adjoint representations. Using the SW-map, Calmet *et al.*[9] first constructed a model with noncommutative gauge invariance which was close to the usual commuting standard model(CSM) and is known as the *minimal* noncommutative standard model(mNCSM) in which they listed several Feynman rules comprising NC interaction. Intense phenomenological searches [10] have been made to unravel several interesting features of this mNCSM. Hewett *et al.* explored several processes e.g. $e^+e^- \rightarrow e^+e^-$ (Bhabha), $e^-e^- \rightarrow e^-e^-$ (Möller), $e^-\gamma \rightarrow e^-\gamma$, $e^+e^- \rightarrow \gamma\gamma$ (pair annihilation), $\gamma\gamma \rightarrow e^+e^-$ and $\gamma\gamma \rightarrow \gamma\gamma$ in the context of NCQED and NCSM. Recently, one of us has investigated the impact of Z and photon exchange in the Bhabha and the Möller scattering, which is reported in [11]. Conroy *et al.*[12] have investigated the process $e^+e^- \rightarrow \gamma \rightarrow \mu^+\mu^-$ in the context of NCQED and predicted a reach of $\Lambda = 1.7$ TeV. In addition to the photon(γ) exchange, we also consider the s -channel exchange of the Z boson. Now in a generic NCQED the triple photon vertex arises to order $\mathcal{O}(\Theta)$, which however is absent in this mNCSM. Another formulation of the NCSM came to the forefront through the pioneering work by Melic *et al.*[13] where such a triple neutral gauge boson coupling [14] appears naturally in the gauge sector. We will call this the nonminimal version of NCSM or simply NCSM. The

Feynman rules to order $\mathcal{O}(\Theta)$ were presented in their work [13]. In 2007, Alboteanu *et al* presented the $\mathcal{O}(\Theta^2)$ Feynman rules for the first time. In the present work we will confine ourselves within this nonminimal version of the NCSM and use the Feynman rules given in Alboteanu *et al.*[15].

The noncommutativity parameter $\Theta_{\mu\nu}$ may be an elementary constant in nature that has a fixed direction in a specific coordinate system fixed, to the celestial sphere. The laboratory frame which is located on the earth, is moving by earth's rotation. So we should take into account the apparent time variation of $\Theta_{\mu\nu}$ in the laboratory frame when we make any phenomenological investigation of scattering or decay on the surface of the earth. In this paper, we consider the effect of earth's rotation (which was not taken into account in one of our earlier work [16]) on the muon pair production in the upcoming Linear Collider.

In addition if spacetime is anisotropic due to the noncommutativity, then a probe to the magnitude of the length scale (scale of anisotropy) and the specific direction of $\Theta_{\mu\nu}$ may be very interesting both from an experimental and theoretical point of view. We may determine the direction of $\Theta_{\mu\nu}$ by studying the behaviour of several time averaged observables.

In Sec II, we describe the parametrization of the noncommutativity parameter $\Theta_{\mu\nu}$ including the effect of earth's rotation. We construct several time-averaged observables i.e. the cross section and the differential cross-section of $e^+e^- \rightarrow \gamma, Z \rightarrow \mu^+\mu^-$. In Sec III, we make a detailed numerical analysis and discuss the prospects of the TeV scale noncommutative geometry. Finally, in Sec IV we summarize our results and conclude.

II. $e^+e^- \rightarrow \mu^+\mu^-$ SCATTERING IN THE LABORATORY FRAME

The muon pair production process $e^-(p_1)e^+(p_2) \rightarrow \mu^-(p_3)\mu^+(p_4)$ proceeds via the s channel exchange of γ and Z bosons in the NCSM, like the standard model. The corresponding Feynman diagrams are shown in Fig. 1. In order to have the cross section to order $\mathcal{O}(\Theta^2)$,

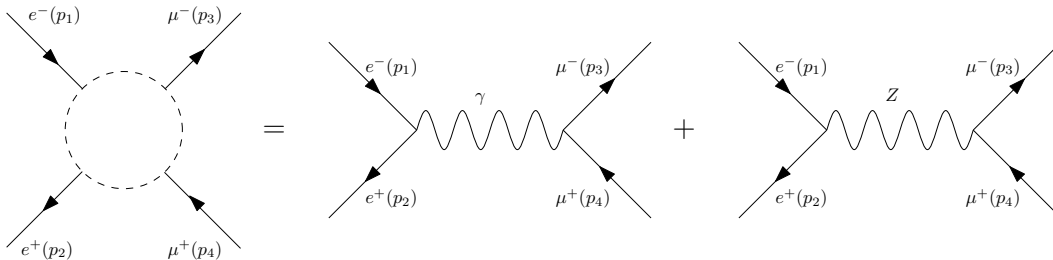


FIG. 1: Feynman diagrams for $e^+e^- \rightarrow \gamma, Z \rightarrow \mu^+\mu^-$ in the NCSM.

we include the order $\mathcal{O}(\Theta^2)$ Feynman rule. The scattering amplitude to order $\mathcal{O}(\Theta^2)$ for the photon mediated diagram can be written as

$$\mathcal{A}_\gamma = \frac{4\pi\alpha}{s} [\bar{v}(p_2)\gamma_\mu u(p_1)] [\bar{u}(p_3)\gamma^\mu v(p_4)] \times \left[\left(1 - \frac{(p_2\Theta p_1)^2}{8}\right) + \frac{i}{2}(p_2\Theta p_1) \right] \times \left[\left(1 - \frac{(p_4\Theta p_3)^2}{8}\right) + \frac{i}{2}(p_4\Theta p_3) \right] \quad (9)$$

and the same for the Z boson mediated diagram as

$$\mathcal{A}_Z = \frac{\pi\alpha}{\sin^2(2\theta_W)s_Z} [\bar{v}(p_2)\gamma_\mu(a + \gamma^5)\bar{u}(p_1)] \times [\bar{u}(p_3)\gamma^\mu(a + \gamma^5)v(p_4)] \times \left[\left(1 - \frac{(p_2\Theta p_1)^2}{8}\right) + \frac{i}{2}(p_2\Theta p_1) \right] \times \left[\left(1 - \frac{(p_4\Theta p_3)^2}{8}\right) + \frac{i}{2}(p_4\Theta p_3) \right] \quad (10)$$

where $s = (p_1 + p_2)^2$, $\alpha = e^2/4\pi$, $a = 4\sin^2(\theta_W) - 1$ and θ_W is the Weinberg angle. In the above $s_Z = s - m_Z^2 - im_Z\Gamma_Z$, where m_Z and Γ_Z are the mass and decay width of the Z boson. The Feynman rules required to evaluate such processes are listed in Appendix A.

Since the noncommutative parameter $\Theta_{\mu\nu}$ is considered as fundamental constant in nature, it's direction is fixed with respect to an inertial(non rotating) coordinate system (which can be a celestial coordinate system). Now the experiment is done in the laboratory coordinate system which is located on the surface of the earth and is moving by the earth's rotation. This results in an aparent time variation of $\Theta_{\mu\nu}$ which should be taken into account before making any phenomenological investigations.

The effect of earth's rotation on noncommutative phenomenology were considered in several earlier studies [17]. Here we follow the work of Kamoshita [17]. Let \hat{e}_X , \hat{e}_Y and \hat{e}_Z be the orthonormal basis of the primary(non rotating) coordinate system (X-Y-Z). Then in the laboratory coordinate system ($\hat{i} - \hat{j} - \hat{k}$) the bases vectors of the primary(non rotating) coordinate system can be written as

$$\hat{e}_X = \begin{pmatrix} c_a s_\zeta + s_\delta s_a c_\zeta \\ c_\delta c_\zeta \\ s_a s_\zeta - s_\delta c_a c_\zeta \end{pmatrix}, \hat{e}_Y = \begin{pmatrix} -c_a c_\zeta + s_\delta s_a s_\zeta \\ c_\delta s_\zeta \\ -s_a c_\zeta - s_\delta c_a s_\zeta \end{pmatrix}, \hat{e}_Z = \begin{pmatrix} -c_\delta s_a \\ s_\delta \\ c_\delta c_a \end{pmatrix}.$$

Here we have used the abbreviations $c_\beta = \cos\beta$, $s_\beta = \sin\beta$ etc. In Fig. 2 we have shown the primary($X - Y - Z$) and laboratory($x - y - z$) coordinate system. Note that the primary Z axis is along the axis of earth's rotation and (δ, a) defines the location of $e^- - e^+$ experiment on the earth, with $-\pi/2 \leq \delta \leq \pi/2$ and $0 \leq a \leq 2\pi$. Because of earth's rotation the angle ζ

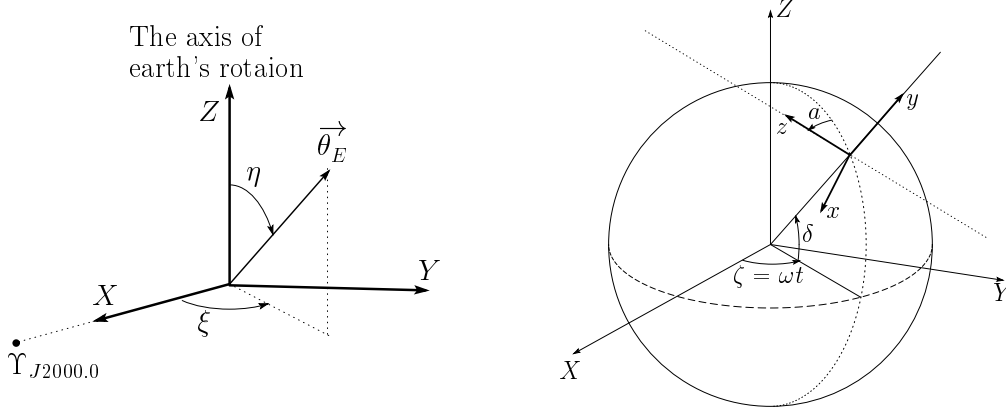


FIG. 2: In the left figure the primary coordinate system(X - Y - Z) is shown. The electric field component $\vec{\Theta}_E$ of $\Theta_{\mu\nu}$ is shown with $\eta(= \eta_E)$ and $\xi(= \xi_E)$, respectively the polar and the azimuthal angle. On the right figure the arrangement of laboratory coordinate system (x - y - z) for an experiment on the earth in the primary coordinate system (X - Y - Z) is shown. In above $\zeta = \omega t$ where ω is a constant. Also (δ, a) , which defines the location of the laboratory, are constants.

(see Fig. 2) increases with time and the detector comes to its original position after a cycle of one complete day, one can define $\zeta = \omega t$ with $\omega = 2\pi/T_{day}$ and $T_{day} = 23h56m4.09053s$. Thus the electric and the magnetic components of the NC parameter $\Theta_{\mu\nu}$ in the laboratory frame is given by

$$\begin{aligned}\vec{\Theta}_E &= \Theta_E(\sin \eta_E \cos \xi_E \hat{e}_X + \sin \eta_E \sin \xi_E \hat{e}_Y + \cos \eta_E \hat{e}_Z) \\ \vec{\Theta}_B &= \Theta_B(\sin \eta_B \cos \xi_B \hat{e}_X + \sin \eta_B \sin \xi_B \hat{e}_Y + \cos \eta_B \hat{e}_Z)\end{aligned}\tag{11}$$

with

$$\vec{\Theta}_E = (\Theta^{01}, \Theta^{02}, \Theta^{03}), \quad \vec{\Theta}_B = (\Theta^{23}, \Theta^{31}, \Theta^{12})\tag{12}$$

and

$$\Theta_E = |\vec{\Theta}_E| = 1/\Lambda_E^2, \quad \Theta_B = |\vec{\Theta}_B| = 1/\Lambda_B^2.\tag{13}$$

Here (η, ξ) specifies the direction of the NC parameter $\Theta_{\mu\nu}$ w.r.t the primary coordinate system with $0 \leq \eta \leq \pi$ and $0 \leq \xi \leq 2\pi$. In above Θ_E and Θ_B are the model parameters and the corresponding energy scale are defined by $\Lambda_E = 1/\sqrt{\Theta_E}$ and $\Lambda_B = 1/\sqrt{\Theta_B}$ which one can probe for different processes.

The spin-averaged squared-amplitude is given by

$$|\overline{\mathcal{A}}|^2 = |\overline{\mathcal{A}_\gamma}|^2 + |\overline{\mathcal{A}_Z}|^2 + 2\text{Re}(\overline{\mathcal{A}_\gamma \mathcal{A}_Z^\dagger}). \quad (14)$$

The different terms in Eq. 14 are given in Appendix C. In order to calculate several squared-amplitude terms we use the Feynman rule to order $\mathcal{O}(\Theta^2)$. Interestingly we found that all lower order terms, i.e. $\mathcal{O}(\Theta)$, $\mathcal{O}(\Theta^2)$, and $\mathcal{O}(\Theta^3)$, get cancelled (see Appendixes C and D for further discussions). Since it is difficult to get the time dependent data, we take the average of the cross section or their distribution over the sidereal day T_{day} and compare that with the experimental data. We introduce the time averaged observables as follows:

$$\left\langle \frac{d^2\sigma}{d\cos\theta d\phi} \right\rangle_T = \frac{1}{T_{day}} \int_0^{T_{day}} \frac{d\sigma}{d\cos\theta d\phi} dt, \quad (15)$$

$$\left\langle \frac{d\sigma}{d\cos\theta} \right\rangle_T = \frac{1}{T_{day}} \int_0^{T_{day}} \frac{d\sigma}{d\cos\theta} dt, \quad (16)$$

$$\left\langle \frac{d\sigma}{d\phi} \right\rangle_T = \frac{1}{T_{day}} \int_0^{T_{day}} \frac{d\sigma}{d\phi} dt, \quad (17)$$

$$\langle \sigma \rangle_T = \frac{1}{T_{day}} \int_0^{T_{day}} \sigma dt, \quad (18)$$

where

$$\sigma = \int_{-1}^1 d(\cos\theta) \int_0^{2\pi} d\phi \frac{d\sigma}{d\cos\theta d\phi}, \quad (19)$$

$$\frac{d\sigma}{d\cos\theta} = \int_0^{2\pi} d\phi \frac{d\sigma}{d\cos\theta d\phi}, \quad (20)$$

$$\frac{d\sigma}{d\phi} = \int_{-1}^1 d(\cos\theta) \frac{d\sigma}{d\cos\theta d\phi}. \quad (21)$$

In the above

$$\frac{d^2\sigma}{d\cos\theta d\phi} = \frac{1}{64\pi^2 s} |\overline{\mathcal{A}}|^2, \quad (22)$$

where $\sigma = \sigma(\sqrt{s}, \Lambda, \theta, \phi, t)$. The time dependence in the cross section or its distribution enters through the NC parameter $\vec{\Theta} (= \vec{\Theta}_E)$ which changes with the change in $\zeta = \omega t$. The angle parameter ξ appears in the expression of $\vec{\Theta}$ through $\cos(\omega t - \xi)$ or $\sin(\omega t - \xi)$ [17] as the initial phase for time evolution which disappears in time averaged observables. So one can deduce $\vec{\Theta}_E$ i.e. Λ_E and the angle η_E from the time-averaged observables.

III. NUMERICAL ANALYSIS

We describe in detail several characteristic results of the muon pair production in the NCSM and discuss how to probe the NC scale $\vec{\Theta}_E$ using observables in the laboratory

coordinate system. Since it is difficult to get the time-dependent data, we consider the time-averaged total and differential cross-section and investigate their sensitivity on Λ ($= \Lambda_E$) and η ($= \eta_E$). We set the laboratory coordinate system by taking $(\delta, a) = (\pi/4, \pi/4)$ which is the OPAL experiment at LEP.

A. Time-averaged angular distribution

The angular distribution of the final state scattered particles is a useful tool to understand the nature of new physics. Since the noncommutativity of space-time defined by Eq. (1) breaks Lorentz invariance including rotational invariance around the beam axis, this will lead to an anisotropy in the azimuthal distribution of the cross section i.e. the distribution will depend on ϕ . This anisotropy which persists in the time-averaged (averaged over the sidereal day T_d) azimuthal distribution of the cross section $\langle \frac{d\sigma}{d\phi} \rangle_T$, can act as a clear signature of space time noncommutativity that is absent in the Standard Model and in many other extensions of it.

In Fig. 3 on the l.h.s we have plotted $\langle \frac{d\sigma}{d\phi} \rangle_T$ vs the azimuthal angle ϕ for different values of η . We set the machine energy $\sqrt{s}(= E_{com}) = 1.5$ TeV and the NC scale Λ at 0.8 TeV.

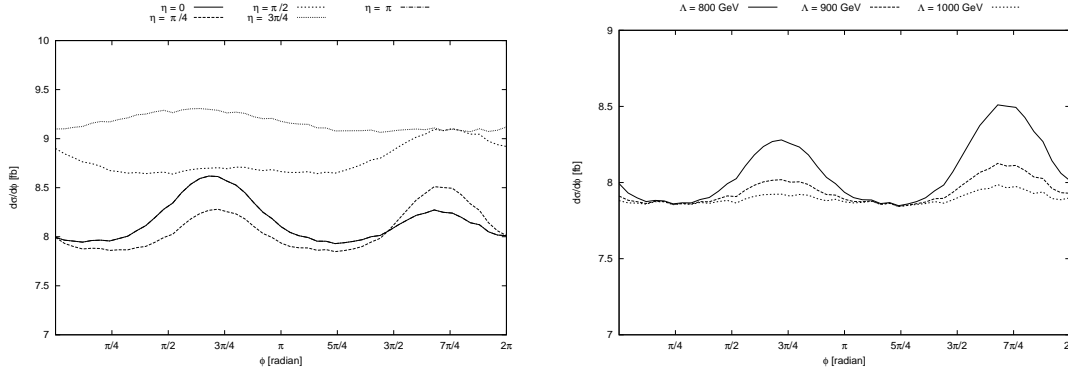


FIG. 3: On the left $\langle \frac{d\sigma}{d\phi} \rangle_T$ is plotted as a function of ϕ for $\eta = 0, \pi/4, \pi/2, 3\pi/4$ and π . We set the scale $\Lambda = 0.8$ TeV. On the right $\langle \frac{d\sigma}{d\phi} \rangle_T$ is plotted as a function of ϕ corresponding to $\Lambda = 0.8, 0.9$ and 1.0 TeV and $\eta = \pi/4$. For both plots we set the machine energy $E_{com} = 1.5$ TeV.

The distribution has peaks corresponding to $\eta = 0, \pi/4, \pi/2$ and π . The plots on the l.h.s corresponding to $\eta = 0$ and π are coincident. For $\eta = \pi/4$ the peak at the left (located at $\phi = 3\pi/4$) is smaller than the peak at the right (located at $\phi = 7\pi/4$) which is quite pronounced. For $\eta = 0$ and π it is opposite. The plot corresponding to $\eta = \pi/2$ has a smaller peak at $\phi = 7\pi/4$, whereas the plot corresponding to $\eta = 3\pi/4$ is almost flat. On

the r.h.s of Fig. 3, we have plotted $\left\langle \frac{d\sigma}{d\phi} \right\rangle_T$ as a function of ϕ with $\Lambda = 0.8, 0.9$ and 1.0 TeV. We set $\eta = \pi/4$ and $E_{com} = 1.5$ TeV. Clearly the plot shows that there are two peaks: one at $\phi = 3\pi/4$ and the other at $\phi = 7\pi/4$. The height of the peaks increases as one changes Λ from 1.0 TeV to 0.8 TeV. Also the peaks on the right of a given plot are bigger than the ones on the left. This clearly shows the sensitivity of the distribution(signal) on the orientation (η) of the NC vector $\vec{\Theta}_E$, the orientation of the LC detector and the NC scale Λ .

Next we consider the polar distribution $\left\langle \frac{d\sigma}{d\cos\theta} \right\rangle_T$. In Fig. 4 we have plotted $\left\langle \frac{d\sigma}{d\cos\theta} \right\rangle_T$ as a function of $\cos\theta$, θ being the scattering angle of the final state muon(μ^-). On the l.h.s figure the plots correspond to $\Lambda = 0.8$ TeV and $\eta = 0, \pi/4, \pi/2, 3\pi/4$ and π , respectively. No significant changes in the polar distribution with η is found. On the r.h.s figure we have shown the plot of $\left\langle \frac{d\sigma}{d\cos\theta} \right\rangle_T$ as a function of $\cos\theta$ with $\eta = \pi/4$ and $\Lambda = 0.8, 0.9$ and 1.0 TeV. So the time-averaged polar distribution is found to be insensitive to the orientation angle η and the NC scale Λ .

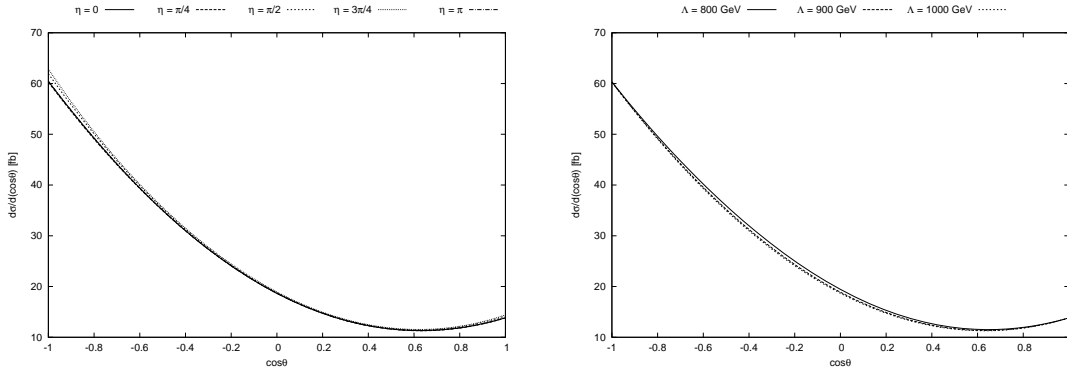


FIG. 4: On the left $\left\langle \frac{d\sigma}{d\cos\theta} \right\rangle_T$ is plotted against $\cos\theta$ corresponding to the NC scale $\Lambda = 0.8$ TeV and the orientation angle $\eta = 0, \pi/4, \pi/2, 3\pi/4$ and π . On the right $\left\langle \frac{d\sigma}{d\cos\theta} \right\rangle_T$ is plotted against $\cos\theta$ for $\Lambda = 0.8, 0.9$ and 1.0 TeV and $\eta = \pi/4$. For both plots the machine energy is chosen to be $E_{com} = 1.5$ TeV.

B. Time averaged total cross section

In Fig. 5 we have plotted the time-averaged total cross-section $\langle \sigma_T \rangle_T$ (in fb) as a function of the machine energy E_{com} (see the plots on the left) which varies from 0.5 TeV to 2 TeV. The three curves corresponding to $\Lambda = 0.8, 0.9, 1.0$ TeV and $\eta = \pi/4$ looks almost same: no significant deviation among them is found until the energy reaches 1.5 TeV. On the right we have plotted the same with the machine energy(E_{com}) varying from 1.5 to $E_{com} = 2.0$ TeV. We see a significant enhancement in the cross-section with the decrease in Λ . In Table

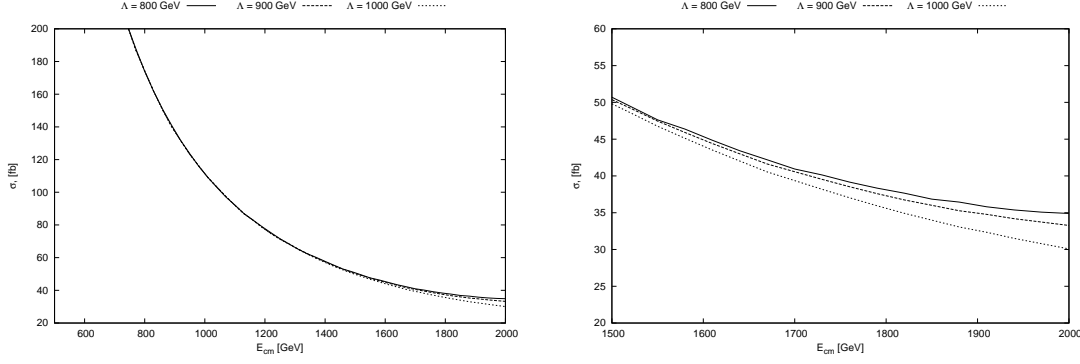


FIG. 5: On the left the time-averaged total cross-section $\langle\sigma_T\rangle_T$ (fb) is plotted as a function of E_{com} corresponding to $\eta = \pi/4$ and $\Lambda = 0.8, 0.9$ and 1.0 TeV. On the right the same quantity is plotted corresponding to $E_{com} = 1.5$ TeV to $E_{com} = 2.0$ TeV.

1, we make an estimate of the number of events per year (say, N) corresponding to different Λ . We set the machine energy E_{com} at 1.5 TeV and 2.0 TeV with the integrated luminosity $\mathcal{L} = 100 \text{ fb}^{-1}$ for the LC. We see that N varies from 5100 yr^{-1} to 5000 yr^{-1} corresponding to $E_{com} = 1.5$ TeV and from 3500 yr^{-1} to 3000 yr^{-1} for $E_{com} = 2.0$ TeV as Λ changes from 0.8 TeV to 1.0 TeV.

Table 1

| Λ (GeV) | NC signal (σ)(fb) | $\mathcal{L}(\text{fb}^{-1})$ | N (events per year) |
|-----------------|----------------------------|-------------------------------|---------------------|
| 800 | 51 (35) | 100 | 5100 (3500) |
| 900 | 51 (33) | 100 | 5100 (3300) |
| 1000 | 50 (30) | 100 | 5000 (3000) |

Table 1: Progressive reduction of the NC signal and the number of events per year with the increase in Λ . We set the machine energy $E_{com} = 1.5$ TeV (2.0 TeV). We choose $\eta = \pi/4$ and the integrated luminosity of the LC about $\mathcal{L} = 100 \text{ fb}^{-1} \text{ yr}^{-1}$.

C. Time averaged total cross section as a function of η

In Fig. 6 we have plotted $\langle\sigma_T\rangle_T$ (time averaged total cross section) as a function of η corresponding to $E_{com} = 1.5$ TeV and the NC scale $\Lambda = 0.8, 0.9$ and 1.0 TeV. The plot shows that the cross-section has peaks at $\eta = 0.659\pi$: the peak corresponding to $\Lambda = 0.8$ TeV is quite pronounced. The height of the peak decreases (and thus the NC signal) with the increase of Λ from 0.8 TeV to 1.0 TeV.

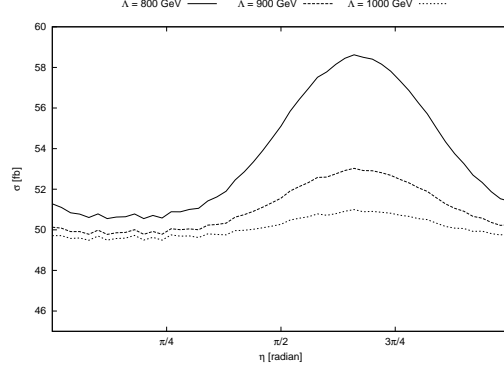


FIG. 6: The time-averaged cross-section $\langle \sigma_T \rangle_T$ (fb) is plotted as a function of η with the machine energy $E_{com} = 1.5$ TeV and the NC scale $\Lambda = 0.8, 0.9$ and 1.0 TeV, respectively. There are some characteristic peaks in the plot which are located at $\eta = 0.659\pi$.

D. Time varying total cross section

Finally we look at the time dependent behaviour of the cross-section. In Fig. 7 we have plotted σ (unaveraged) as a function of $\zeta(= \omega t - \xi)$ corresponding to $\eta = 0, \pi/4, \pi/2, 3\pi/4$ and π . Here $\omega = 2\pi/T_{day}$ with $T_{day} = 23h56m4.09053s$. We set the machine energy $E_{com} = 1.5$ TeV, $\Lambda = 0.8$ TeV and $\xi = 0$ in ζ . We make the following observations:

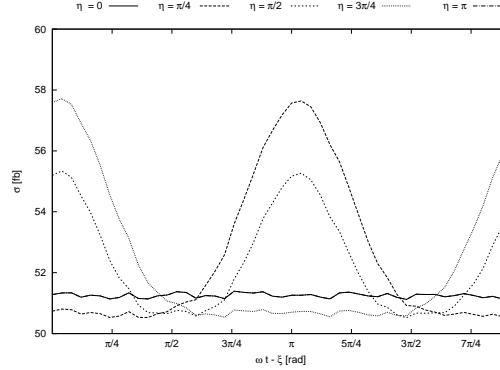


FIG. 7: The total cross section σ is plotted as a function of $\zeta(= \omega t - \xi)$ (with $\xi = 0$) corresponding to $\eta = 0, \pi/4, \pi/2, 3\pi/4$ and π . We set $E_{com} = 1.5$ TeV and $\Lambda = 0.8$ TeV. There are peaks in the plot corresponding to $\eta = \pi/4$ and $\pi/2$ which are located at $\zeta = 3.27$ rad.

- The cross section σ is found to be completely flat for $\eta = 0$ and π : no change in the cross section as a function of ζ over the period of the complete day T_{day} .
- The cross-section σ has a pronounced peak at $\omega t = 3.27$ rad corresponding to $\eta = \pi/4$. Beyond this particular ζ it falls everywhere. Similarly, the cross-section corresponding to $\eta = 3\pi/4$ shows exactly the opposite behaviour obtained for $\eta = \pi/4$. At $\omega t = 3.27$

rad it is found to be flat, whereas on either side it increases and possesses maximum at $\omega t = 0.12$ rad and 6.28 rad, respectively.

- Finally we see that the unaveraged cross section σ (corresponding to $\eta = \pi/2$) have alternate maxima and minima which at $t = 0.12/\omega$, $3.27/\omega$ and $6.28/\omega$ sec i.e. different times of a day. This periodic cross-section (and thus the signal) is quite interesting and the finding of such event at the Linear Collider will validate the idea of the space-time noncommutativity at the TeV scale.

IV. CONCLUSION

We have investigated the effect of space-time noncommutativity on the fundamental processes $e^+e^- \rightarrow \gamma, Z \rightarrow \mu^+\mu^-$ taking the earth rotation into account. With the $\mathcal{O}(\Theta^2)$ Feynman rules, we found that the $\mathcal{O}(\Theta)$, $\mathcal{O}(\Theta^2)$ and $\mathcal{O}(\Theta^3)$ contributions to the cross section get canceled and the nonvanishing lowest order contribution to be $\mathcal{O}(\Theta^4)$. Since it is difficult to get time-dependent data, we have constructed several time-averaged observables and investigated their sensitivities on the NC scale $\Lambda (= \Lambda_E)$ and the orientation (polar) angle $\eta (= \eta_E)$ of the electric NC vector (since the muon pair production is found to be sensitive to only the electric $\vec{\Theta}_E$ vector). The pronounced peaks observed in the time-averaged azimuthal distribution are located at $\phi = 3\pi/4$ and $7\pi/4$ corresponding to the machine energy $E_{com} = 1.5$ TeV, $\Lambda = 0.8$ TeV and $\eta = 0, \pi/4, \pi/2$ and π . These peaks which are not there in the standard model and in many other models (beyond the standard model), can act as the clear signature of space-time noncommutativity. We find that the NC signal in the azimuthal distribution gets enhanced with the decrease in the NC scale Λ . The polar distribution (time-averaged) is found to be insensitive to Λ and η . However the asymmetry around the $\cos \theta = 0$ persists even when the space-time is noncommutative. We have found σ (time-averaged total cross-section) as a function of the machine energy E_{com} . Assuming the integrated luminosity of LC about 100 fb^{-1} , we find that the number of events varies from 5100 yr^{-1} to 5000 yr^{-1} as the NC scale Λ changes from 1 TeV to 0.8 TeV at a machine energy $E_{com} = 1.5$ TeV. We have also shown the dependence of the time-averaged total cross-section $\langle \sigma_T \rangle_T$ on the orientation angle η of the NC vector corresponding to the machine energy $E_{com} = 1.5$ TeV and $\Lambda = 0.8, 0.9$ and 1.0 TeV, respectively. It clearly shows pronounced peak at $\eta = 0.659 \pi$: which clearly establish the sensitivity of $\langle \sigma_T \rangle_T$ on η . Finally, we have shown the variation of

the total cross-section $\sigma(\text{unaveraged})$ as a function of $\zeta(=\omega t - \xi)$ (with $\xi = 0$). At certain times of a day the cross-section and the NC signal becomes maximum. Corresponding to $\eta = \pi/4$, we find that the cross-section is maximum at $\omega t = 3.27$ rad, whereas for $\eta = 3\pi/4$ it appears at $\omega t = 0.12$ rad and 6.28 rad, respectively. The cross-section σ corresponding to $\eta = \pi/2$ is seen to have alternate maxima and minima which appears during different times of a day. The periodic appearance of maxima and minima of the NC signal is a novel prediction which can be tested in the upcoming Linear Collider. Thus the noncommutative geometry is quite rich in terms of its phenomenological implications and it is worthwhile to explore several other interesting processes, potentially relevant for the future Linear Collider.

Acknowledgments

The work of P.K.Das is supported by the SEED Project 2011 and DST YS Project SR/FTP/PS-11/2006. The authors would like to acknowledge Mr. Anupam Mitra who was involved in the initial part of this project. P.K.Das would like to thank Santosh Kumar Rai of Oklahoma University, USA for his useful comments.

Appendix A: Feynman rules to order $\mathcal{O}(\Theta^2)$

Following Ref. [15], the Feynman rule for the $f(p_{in}) - f(p_{out}) + \gamma(k)$ vertex (where f represents a fermion) to $\mathcal{O}(\Theta^2)$ can be written as $igV_\mu(p_{out}, k, p_{in})$, where

$$V_\mu^{(1)}(p_{out}, k, p_{in}) = \frac{i}{2}[(k\Theta)_\mu \not{p}_{in}(1 - 4c_\psi^{(1)}) + 2(k\Theta)_\mu(c_A^{(1)} - c_\psi^{(1)}) - (p_{in}\Theta)_\mu \not{k} - (k\Theta p_{in})\gamma_\mu]. \quad (\text{A1})$$

$$V_\mu^{(2)}(p_{out}, k, p_{in}) = \frac{1}{8}(k\Theta p_{in})[(k\Theta)_\mu \not{p}_{in}(1 - 16c_\psi^{(2)}) + 4(k\Theta)_\mu(c_A^{(1)} - 2c_\psi^{(2)}) - (p_{in}\Theta)_\mu \not{k} - (k\Theta p_{in})\gamma_\mu]. \quad (\text{A2})$$

The same for the vertex $f(p_{in}) - f(p_{out}) + Z(k)$ can be obtained by making the necessary substitutions of $\gamma_\mu \longrightarrow g_V\gamma_\mu - g_A\gamma_\mu\gamma_5$. Here $\Theta_{\mu\nu\rho} = \Theta_{\mu\nu}\gamma_\rho + \Theta_{\nu\rho}\gamma_\mu + \Theta_{\rho\mu}\gamma_\nu$, $p_{out}\Theta p_{in} = p_{out}^\mu\Theta_{\mu\nu}p_{in}^\nu = -p_{in}\Theta p_{out}$. In our analysis, we set $c_A^{(1)} = c_\psi^{(1)} = c_\psi^{(2)} = 0$.

The momentum conservation reads as $p_{in} + k = p_{out}$.

Appendix B: Momentum prescriptions and dot products

Working in the center of momentum frame and ignoring electron and muon masses, we can specify the 4 momenta of the particles as follows:

$$p_1 = \left(\frac{\sqrt{s}}{2}, 0, 0, \frac{\sqrt{s}}{2} \right) \quad (\text{B1})$$

$$p_2 = \left(\frac{\sqrt{s}}{2}, 0, 0, -\frac{\sqrt{s}}{2} \right) \quad (\text{B2})$$

$$p_3 = \left(\frac{\sqrt{s}}{2}, \frac{\sqrt{s}}{2} \sin \theta \cos \phi, \frac{\sqrt{s}}{2} \sin \theta \sin \phi, \frac{\sqrt{s}}{2} \cos \theta \right) \quad (\text{B3})$$

$$p_4 = \left(\frac{\sqrt{s}}{2}, -\frac{\sqrt{s}}{2} \sin \theta \cos \phi, -\frac{\sqrt{s}}{2} \sin \theta \sin \phi, -\frac{\sqrt{s}}{2} \cos \theta \right), \quad (\text{B4})$$

where θ is the scattering angle made by the 3-momentum vector p_3 of $\mu^-(p_3)$ with the +ve Z axis and ϕ is the azimuthal angle.

The antisymmetric NC tensor $\Theta_{\mu\nu} = (\vec{\Theta}_E, \vec{\Theta}_B)$ i.e. it has 3 electric and 3 magnetic components. The muon pair production is sensitive to $\vec{\Theta}_E$ and thus one obtain constraints on Λ_E (say, Λ). In the laboratory frame (with $\eta = \eta_E$, $\xi = \xi_E$ (see the earlier discussion))

$$\begin{aligned} \vec{\Theta}_E &= \Theta_E \sin \eta \cos \xi \hat{e}_X + \Theta_E \sin \eta \sin \xi \hat{e}_Y + \Theta_E \cos \eta \hat{e}_Z \\ &= \Theta_{Ex}^{lab} \hat{x} + \Theta_{Ey}^{lab} \hat{y} + \Theta_{Ez}^{lab} \hat{z} \end{aligned} \quad (\text{B5})$$

where

$$\begin{aligned} \Theta_{Ex}^{lab} &= \Theta_E (s_\eta c_\xi (c_a s_\zeta + s_\delta s_a c_\zeta) + s_\eta s_\xi (-c_a c_\zeta + s_\delta s_a s_\zeta) - c_\eta c_\delta s_a) \\ \Theta_{Ey}^{lab} &= \Theta_E (s_\eta c_\xi c_\delta c_\zeta + s_\eta s_\xi c_\delta s_\zeta + c_\eta s_\delta) \\ \Theta_{Ez}^{lab} &= \Theta_E (s_\eta c_\xi (s_a s_\zeta - s_\delta c_a c_\zeta) - s_\eta s_\xi (s_a c_\zeta + s_\delta c_a s_\zeta) + c_\eta c_\delta c_a) \end{aligned} \quad (\text{B6})$$

and

$$\Theta_E = |\vec{\Theta}_E| = 1/\Lambda^2. \quad (\text{B7})$$

In above we have used the abbreviations $s_\eta = \sin \eta$, $c_\eta = \cos \eta$ etc. Here (η, ξ) specifies the direction of the NC parameter ($\vec{\Theta}_E$) w.r.t the primary coordinate system with $0 \leq \eta \leq \pi$ and $0 \leq \xi \leq 2\pi$. Using these in the laboratory frame we find

$$p_2 \Theta p_1 = -\frac{s}{2} \Theta_{Ez}^{lab}, \quad (\text{B8})$$

$$p_4 \Theta p_3 = -\frac{s}{2} (s_\theta c_\phi \Theta_{Ex}^{lab} + s_\theta s_\phi \Theta_{Ey}^{lab} + c_\theta \Theta_{Ez}^{lab}). \quad (\text{B9})$$

where Θ_{Ex}^{lab} , Θ_{Ey}^{lab} and Θ_{Ez}^{lab} are defined above.

Appendix C: Spin-averaged squared-amplitude for $e^+e^- \rightarrow \mu^+\mu^-$

The squared-amplitude terms of Eq.14 are

$$\overline{|\mathcal{A}|^2} = \overline{|\mathcal{A}_\gamma|^2} + \overline{|\mathcal{A}_Z|^2} + 2\overline{Re(\mathcal{A}_\gamma\mathcal{A}_Z^\dagger)} = \frac{1}{4}|\mathcal{A}|^2. \quad (C1)$$

The various components of the squared-matrix element [Eq. 14] are found to be

$$\overline{|\mathcal{A}_\gamma|^2} = \frac{128\pi^2\alpha^2 A_{NC}}{s^2} [(p_1 \cdot p_3)(p_2 \cdot p_4) + (p_1 \cdot p_4)(p_2 \cdot p_3)], \quad (C2)$$

$$\overline{|\mathcal{A}_Z|^2} = \frac{8\pi^2\alpha^2 A_{NC}}{\sin^4(2\theta_W) s_Z^2} [T_1(p_1 \cdot p_4)(p_2 \cdot p_3) + T_2(p_1 \cdot p_3)(p_2 \cdot p_4)], \quad (C3)$$

$$2\overline{Re(\mathcal{A}_Z\mathcal{A}_\gamma^\dagger)} = \frac{64\pi^2\alpha^2 A_{NC}}{\sin^2(2\theta_W)} \frac{1}{s} \frac{(s - m_Z^2)}{s_Z^2} [T_3(p_1 \cdot p_3)(p_2 \cdot p_4) + T_4(p_1 \cdot p_4)(p_2 \cdot p_3)], \quad (C4)$$

where $s_Z^2 = [(s - m_Z^2)^2 + \Gamma_Z^2 m_Z^2]$, $T_1 = 1 + 6(4s_W^2 - 1)^2 + (4s_W^2 - 1)^4$, $T_2 = 1 - 2(4s_W^2 - 1)^2 + (4s_W^2 - 1)^4$, $T_3 = -1 + (4s_W^2 - 1)^2$ and $T_4 = (4s_W^2 - 1)^2 + 1$. In the above, one finds

$$\begin{aligned} A_{NC} &= \left[\left(1 - \frac{(p_2 \Theta p_1)^2}{8}\right)^2 + \frac{(p_2 \Theta p_1)^2}{4} \right] \left[\left(1 - \frac{(p_4 \Theta p_3)^2}{8}\right)^2 + \frac{(p_4 \Theta p_3)^2}{4} \right] \\ &= \left[1 + \frac{(p_2 \Theta p_1)^4}{64} \right] \left[1 + \frac{(p_4 \Theta p_3)^4}{64} \right] \end{aligned} \quad (C5)$$

Interestingly, the inclusion of the order $\mathcal{O}(\Theta^2)$ Feynman rule leads to the cancellation of all lower order terms. A relevant discussion is made at the end of this appendix and in the next appendix.

Equations C2 - C4 can be rewritten using the results and prescriptions of Appendix B as

$$\overline{|\mathcal{A}_\gamma|^2} = 16\pi^2\alpha^2(1 + \cos^2\theta) \times A_{NC} \quad (C6)$$

$$\overline{|\mathcal{A}_Z|^2} = \frac{4\pi^2\alpha^2}{\sin^4(2\theta_W)} \frac{s^2}{[(s - m_Z^2)^2 + \Gamma_Z^2 m_Z^2]} [(1 - 4s_W^2 + 8s_W^4)^2(1 + \cos^2\theta) + 2(1 - 4s_W^2)^2 \cos\theta] \times A_{NC} \quad (C7)$$

$$2\overline{Re(\mathcal{A}_Z\mathcal{A}_\gamma^\dagger)} = \frac{8\pi^2\alpha^2}{\sin^2(2\theta_W)} \frac{s(s - m_Z^2)}{[(s - m_Z^2)^2 + \Gamma_Z^2 m_Z^2]} [(1 - 4s_W^2)^2(1 + \cos^2\theta) + 2 \cos\theta] \times A_{NC} \quad (C8)$$

where $s_W = \sin\theta_W$.

Appendix D: A note on the order by order (in Θ) vanishing contribution to the cross section

The process that we are considering is a single s -channel process and interestingly the inclusion of $\mathcal{O}(\Theta^2)$ terms in the matter-gauge boson interaction vertex, leads to the cancellation of all lower order $\mathcal{O}(\Theta, \Theta^2, \Theta^3)$ terms in the cross section. The contribution (nonvanishing) to the cross section discussed so far is $\mathcal{O}(\Theta^4)$ ($\mathcal{O}(1/\Lambda^8)$). It should be recognized that an accurate description, as a result of the cancellation would now require Feynman rules to all orders. In fact, it is quite likely that such cancellations successively continue even with the higher order terms, ultimately resulting in no net effect from space-timennoncommutivity! This was shown in a work by Hewett *et al.*[10] where the effect merely pulls out as an overall phase factor. However, these remain only speculative due to the unavailability and inherent difficulty in generating higher order Feynman rules. In any case, we believe that the work presented in this paper throws light on crucial aspects with regard to NCSM– not only in demonstrating the nature of subtle modifications in the distribution curves, but also in demonstrating that such effects in a single channel process can in fact successively negate, resulting in no net effect and rendering the traditional perturbative approach ineffective.

-
- [1] N. Arkani-Hamed, S. Dimopoulos and G. Dvali, *Phys. Lett. B* **429** , 263 (1998); I. Antoniadis, N. Arkani-Hamed and G. Dvali, *Phys. Lett. B* **463**, 257 (1998).
 - [2] H.S. Snyder, *Phys. Rev. D* **71**, 38 (1947).
 - [3] A.Connes,M.R.Douglas and A.Schwarz, *J. High Energy Phys.* 02 (1998) 003.
 - [4] M.R.Douglas and C.Hull, *J. High Energy Phys.* **02**(1998) 008.
 - [5] N. Seiberg and E. Witten, *J. High Energy Phys.* **09**(1999) 032.
 - [6] E.Witten, *Nucl. Phys.* **B471**,135(1996); P.Horava and E.Witten, *Nucl. Phys.* **B460**,506(1996).
 - [7] M. R. Douglas and N. Nekrasov, *Rev. Mod. Phys.* **73**, 977 (2001); I. F. Riad and M. M. Sheikh-Jabbari, *J. High Energy Physics* **08**, 45 (2000); B. Jurco and P. Schupp, *Eur. Phys. J. C* **14**, 367 (2000).
 - [8] B. Jurco, P. Schupp and J. Wess, *Mod. Phys. Lett.* **A16**, 343 (2001).
 - [9] X. Calmet, B. Jurco, P. Schupp, J. Wess and M. Wohlgenannt, *Eur. Phys. J. C* **23**, 363

- (2002); X. Calmet Eur. Phys. J. C **50**, 113 (2007).
- [10] J.Hewett, F.J.Petriello and T.G.Rizzo, in *Signals for Noncommutative QEC at High Energy e^+e^- colliders*, eConf C010630, E3064 (2001); J.Hewett *et al.*, Phys. Rev. D **64**, 075012 (2001), Phys. Rev. D **66**, 036001 (2002); T. G. Rizzo Int. J. Mod. Phys. **A18**, 2797 (2003); A. Alboteanu, T. Ohl and R. Ruckl, Acta Phys. Pol. B bf 38, 3647 (2007); P. K. Das *et al.*, Phys. Rev. D **77**, 035010 (2008).
- [11] P. K. Das *et al.*, Phys. Rev. D **77**, 035010 (2008).
- [12] J. M. Conroy *et al.*, Phys. Rev. D **68**, 054004 (2003).
- [13] B. Melić, K. P. Kumericki, J. Trampetic, P. Schupp and M. Wohlgenannt Eur. Phys. J. C **42**, 483 (2005);
- [14] G. Duplancic, P. Schupp and J. Trampetic Eur. Phys. J. C **32**, 141 (2003); W. Behr, N. G. Deshpande, G. Duplancic, P. Schupp, J. Trampetic and J. Wess, Eur. Phys. J. C **29**, 441 (2003); P. Aschieri, B. Jurco, P. Schupp and J. Wess Nucl. Phys. **B651**, 45 (2003).
- [15] A. Alboteanu *et al.*, Phys. Rev. D **76**, 105018 (2007).
- [16] P. Abhishodh, A. Mitra and P. K. Das, Phys. Rev. D **82**, 055020 (2010); Phys. Rev. D **83**, 056002 (2011).
- [17] H. Grosse and Y. Liao, Phys. Rev. D **64**, 115007 (2001); J. i. Kamoshita, Eur. Phys. J. C **52**, 451 (2007); M. Haghighat *et al.*, Phys. Rev. D **82**, 016007 (2010); S. K. Garg, T. Shrecharan, P. K. Das, N. G. Deshpande and G. rajasekaran, J. High Energy Physics **1107**, 24 (2011).